Whole-air relaxed eddy accumulation for the measurement of isotope and trace-gas fluxes

by

J. Ruppert, M. Riederer, W. A. Brand and T. Foken

Editorial remarks

This report was part of the PhD-Thesis by J. Ruppert (2009). The paper was not accepted because of the availability of measuring systems based on tunable lasers. Nevertheless the method has significant benefits in relation to the accuracy of the measured fluxes even when the handling is not simple. Therefore, the system was again used in the ongoing PhD-study by M. Riederer and updated in some details. The following report bases on J. Ruppert's paper with some additional remarks and updates by M. Riederer.

Th. Foken

Whole-air relaxed eddy accumulation for the measurement of isotope and trace-gas fluxes

J. Ruppert[1,2], M. Riederer[1], W. A. Brand[3], T. Foken[1]

[1]Department of Micrometeorology, University of Bayreuth, Germany

[2]now: Research Institute of the Cement Industry, Verein Deutscher Zementwerke, Düsseldorf, Germany

[3]Max Planck Institute for Biogeochemistry, Jena, Germany

Abstract

Measuring the isotopic composition of trace gas fluxes can provide additional information on ecosystem gas exchange, when ecosystem processes, like assimilation, discriminate against heavier isotopes. In the case of CO_2 exchange, different mass-balances for bulk CO_2 and its $^{13}CO_2$ or $CO^{18}O$ isotopes can be used to separate respiration from photosynthetic assimilation. Up to now, detectors for direct isotope measurements in the field lack the precision needed for fast eddy covariance (EC) flux measurements. The collection of updraft and downdraft whole-air samples using the relaxed eddy accumulation technique (REA) allows simultaneously determining trace gas concentrations and isotope ratios by high precision laboratory analysis. At the same time whole-air REA relaxes several of the technical problems related to REA sampling on traps.

In tests using air from a tank the complete whole-air REA sampling system and its foil balloon bag reservoirs showed no signs of contamination after cleaning. The standard deviations of $\delta^{13}C$ and $\delta^{18}O$ isotope ratios were only slightly higher than the precision specified for the laboratory analysis procedure. First experiment results showed that isotopic differences (updrafts–downdrafts) were large enough to yield signal to noise ratios greater than five when applying hyperbolic deadbands during REA sampling (HREA). The performance of the instrument and the HREA sampling method are investigated by simulation of the sampling process for bulk CO_2, which serves as proxy scalar.

Measurements by whole-air HREA in combination with high precision isotope analysis can quantify the isofluxes of $^{13}CO_2$ and $CO^{18}O$. Furthermore, additional information is collected on the scalar correlation of bulk CO_2 and its stable isotopes, which represents the relatively short timescale of updrafts and downdrafts in the turbulent exchange above an ecosystem. This information is essential to check the scalar similarity assumptions made in the HREA and EC/flask method for the quantification of isofluxes.

1. Introduction

In recent years, a special interest was to quantify the isotopic composition of CO_2 flux densities above different ecosystems (*Bowling et al.*, 2003a; *Ehleringer et al.*, 2002; *Yakir and da S. L. Sternberg*, 2000). Such measurements provide means for identifying the individual contributions of sources and sinks with different isotopic signature to the CO_2 net ecosystem exchange (NEE) and the rate of internal recycling of CO_2, e.g. in the canopy space of forests (*Lloyd and Farquhar*, 1994; *Lloyd et al.*, 1996; *Yakir and Wang*, 1996). Two different mass-balances for bulk CO_2 and its isotopes can be used to separate respiration from assimilation, which discriminates against $^{13}CO_2$ and $CO^{18}O$ (*Bowling et al.*, 2001; *Wichura et al.*, 2004; *Wichura*, 2009).

Different eddy sampling methods like relaxed eddy accumulation (REA, *Businger and Oncley*, 1990) are commonly used to measure trace gas fluxes in the boundary layer when fast high precision chemical sensors are not available for eddy covariance (EC) flux measurements. Eddy sampling methods are passive in the sense that they do not modify the turbulent gas exchange of the ecosystem. Therefore such measurements are complementary to measurements with enclosures e.g. on individual parts of the ecosystem and can be used for their validation. Measurements of the turbulent exchange above an ecosystem provide information with a spatial integration that can close a gap of scale between isotope studies at leaf or branch scale and atmospheric isotope studies and large scale modeling approaches (*Canadell et al.*, 2000; *Kaplan et al.*, 2002; *Yakir and da S. L. Sternberg*, 2000). This is especially important for the investigation of carbon budgets of forests, because in tall vegetation complex gas exchange processes exist.

The ability to analyze the isotopic signature of the turbulent exchange is mainly limited by the measurement uncertainty regarding the CO_2 isotope ratios at small differences of bulk CO_2 mixing ratios (*Bowling et al.*, 1999a; *Bowling et al.*, 1999b; *Bowling et al.*, 2003b; *Zobitz et al.*, 2006). Most studies on isotope flux measurements above the canopy focus on the evaluation of the ^{13}C-isotope signatures. In general, the difference of isotope signatures in the CO_2 exchange during the day is expected to be larger for ^{18}O-isotopes, because the ^{18}O-isotope signature of CO_2 can equilibrate with ^{18}O-depleted soil water and ^{18}O-enriched leaf water pools (*Yakir and da S. L. Sternberg*, 2000). $CO^{18}O$ isotope fluxes could therefore yield more independent information on assimilation and respiration. However, measurement results presented by *Bowling et al.* (1999a) were less uniform, which might reflect higher temporal and spatial variability of the water pools.

The aim of this study is to present a method for the measurement of $^{13}CO_2$ and $CO^{18}O$ isotope fluxes based on the hyperbolic relaxed eddy accumulation method (HREA) and whole-air sampling. The application of the hyperbolic sampling criteria maximizes scalar concentration differences (*Bowling et al.*, 1999b). Whole-air sampling allows subsequent high precision isotope analysis in a laboratory directly from the accumulated updraft and downdraft air samples (*Bowling et al.*, 2003a). With the construction of a new sampling system we aimed at further improving the accuracy of isotope sampling especially for ^{18}O isotopes. Sample volumes were increased in order to also allow direct and precise analysis of the corresponding bulk CO_2 mixing ratios. The integrity of isotope samples and sampling accuracy was thoroughly tested in the laboratory and in the field by comparison with independent measurements above a spruce forest during the experiment WALDATEM-2003 and above extensively managed grassland during the experiment FORKAST-TP5 in 2010.

The combined information of CO_2 isotope ratios and mixing ratios in updraft and downdraft air samples is used to analyze the scalar correlation, which is a basic assumption in the HREA and EC/flask methods (*Bowling et al.*, 2003a). Based on the measured bulk CO_2, the HREA sampling pro-

cedure and flux determination method are validated as requested by *Bowling et al.* (1999a) and *Kramm et al.* (1999). The methodological performance of HREA is investigated by simulation of the sampling process. However, the effective sampling efficiencies determined from measured bulk CO_2 data are taken into account for the determination of turbulent isofluxes.

2. Theory

In the conditional sampling or relaxed eddy accumulation method (REA) (*Businger and Oncley*, 1990) the turbulent flux is determined from the concentration difference measured in updraft and downdraft air samples. This concentration difference is scaled with the intensity of turbulent vertical mixing measured by the standard deviation of the vertical wind speed σ_w based on the assumption of flux-variance similarity. Because air sampling is not proportional to the vertical wind speed, it is referred to as relaxed sampling. Consequently, REA is an indirect method for flux measurements. It relies on a parameterization in which the so called *b*-factor is determined from a second scalar quantity (proxy scalar) which shows similarity in its atmospheric transport (scalar similarity, (*Ruppert et al.*, 2006b; *Wyngaard and Moeng*, 1992)) and for which the fluctuations of its concentration can be measured in the field with high temporal resolution:

$$F_c = b\sigma_w\left(\overline{c_\uparrow} - \overline{c_\downarrow}\right). \tag{1}$$

F_c is the turbulent flux of the scalar c. $\overline{c_\uparrow}$ and $\overline{c_\downarrow}$ are the average scalar concentrations respectively in updraft and downdraft air samples expressed as dry air mixing ratios.

For the proxy scalar normally F_c is determined by eddy covariance (EC) measurements ($F_c = \overline{w'c'}$), where w' and c' are the fluctuations of the vertical wind speed w and scalar concentration c around their average values. The over bar denotes Reynolds averaging. The proportionality factor b can then be determined for the proxy scalar by rearranging (1) either based on (i) simulation of REA sampling on high frequency scalar time series and its resulting concentration difference $\overline{c_\uparrow} - \overline{c_\downarrow}$ or based on (ii) measured concentration difference from real REA air sampling for the proxy scalar:

$$b = \frac{\overline{w'c'}}{\sigma_w\left(\overline{c_\uparrow} - \overline{c_\downarrow}\right)} \tag{2}$$

Many studies demonstrate the relative stability of average *b*-factors in unstable and moderately stable conditions (*Ammann and Meixner*, 2002; *Baker et al.*, 1992; *Beverland et al.*, 1996a; *Foken et al.*, 1995). Nevertheless, significant variability of *b*-factors for individual 30 min periods is observed, and different factors are discussed (*Gao*, 1995; *Guenther et al.*, 1996; *Oncley et al.*, 1993; *Pattey et al.*, 1993; *Ruppert et al.*, 2006b). Several studies point out, that skewness in the joint frequency distribution (JFD) of w' and c' and structures in the turbulent exchange are causing changes in *b*-factors (*Fotiadi et al.*, 2005; *Katul et al.*, 1996; *Milne et al.*, 2001; *Ruppert et al.*, 2006b). The study by *Ruppert et al.* (2006b) attributes observed variation in the scalar exchange to events at time scales >60 s. This limits the use of a unique *b*-factor for all times and asks for the determination of individual *b*-factors for each sampling period. Under the assumption of scalar similarity, the *b*-factor determined

for a proxy scalar by (2) is used to derive the turbulent flux of the scalar of interest from its measured average concentration difference between updraft and downdraft REA samples $\overline{c_\uparrow} - \overline{c_\downarrow}$ by solving (1).

Application of a wind deadband for small vertical wind speeds, in which no samples are taken, increases the concentration difference between the updraft and downdraft air accumulation reservoirs and thereby the certainty of the flux measurement, especially if chemical sensor resolution is a limiting factor (*Businger and Delany*, 1990; *Delany et al.*, 1991). At the same time, the *b*-factor decreases with the size of the deadband. The wind deadband size H_w is normally defined in reference to the normalized vertical wind speed fluctuations:

$$\left| \frac{w'}{\sigma_w} \right| \leq H_w .$$

(3)

In the hyperbolic relaxed eddy accumulation method (HREA) the deadband rejects not only samples with small fluctuations of the vertical wind speed w' but also samples with small deviations from the mean scalar concentration, which further increases the concentration difference $\overline{c_\uparrow} - \overline{c_\downarrow}$ (*Bowling et al.*, 1999b; *Bowling et al.*, 2003a):

$$\left| \frac{w'c'}{\sigma_w \sigma_c} \right| \leq H_h .$$

(4)

The hyperbolic deadband with the size H_h must be determined online from a proxy scalar measured with high temporal resolution, which again assumes scalar similarity. A deadband reduces the frequency of valve switching during sampling and at the same time, the number of samples used for flux calculation. It also reduce the sensitivity of REA methods to uncertain definition of the mean vertical wind speed w needed for segregating samples in the up and down reservoirs (*Businger and Oncley*, 1990; *Pattey et al.*, 1993). Details on the sampling method and procedures used in this study are described in Section 3. A comparison of general characteristics of eddy sampling methods like REA and HREA and different sources of error for flux determination are presented in a paper by *Ruppert et al.* (2002).

3. Methods and Material

The design of the whole-air REA system goes back to the principles ideas for conditional sampling of trace gases (*Businger and Oncley*, 1990; *Delany et al.*, 1991; *Desjardins*, 1977; *Oncley et al.*, 1993; *Pattey et al.*, 1993) and is based on a design presented by *Bowling et al.* (2003a) in which foil balloon bags serve as intermediate storage for updraft and downdraft air samples at ambient pressure.

3.1. Scalar similarity

The determination of *b*-factors in the REA method and the online definition of a hyperbolic deadband (i.e. in the HREA method) requires the selection of a proxy scalar, which shows good scalar similarity with the scalars of interest. For this study the bulk CO_2 density signal (ρ_{CO2}) of an open path gas analyzer was selected as proxy scalar for the estimation of the scalar intensity of ^{13}C and ^{18}O isotopes[1] of CO_2. The assumption is, that bulk CO_2 density shows sufficient scalar similarity with the unknown fast fluctuations of the CO_2 isotopic composition. A detailed discussion of the effects of scalar similarity in REA flux measurements is presented by *Ruppert et al.* (2006b) and in the diploma thesis of *Hübner* (2010).

We are confident, that the assumption is justified at least for the efficient selection of the strong up- and downdrafts by a hyperbolic deadband, as all CO_2 isotope turbulent exchange is part of the bulk CO_2 turbulent exchange. Also, linear relationships between the $\delta^{13}C$ isotope ratio and bulk CO_2 mixing ratio of whole-air samples collected at timescales down to 500 ms and of REA samples are reported by *Bowling et al.* (1999a; 2001). Nevertheless, if considering the location of sources and sinks in the ecosystem individually for bulk CO_2, $^{13}CO_2$ and $CO^{18}O$, some difference in the scalar exchange should be expected, which might also affect scalar similarity. Less scalar similarity would introduce some error in HREA flux results with a tendency for underestimating the flux (*Ruppert et al.*, 2006b). The assumption of scalar similarity made here is therefore tested by investigating the $\delta^{13}C/CO_2$ and $\delta^{18}O/CO_2$ relations (Section 4.4).

The following sections describe the implemented online turbulence data analysis, the HREA sampling procedures, the whole-air REA system design for high precision isotope and trace-gas sampling and sample analysis.

3.2. Axis rotation and hyperbolic deadband definition

A three-dimensional planar fit rotation matrix was determined based on 1 month of wind velocity data from the sonic anemometer used for eddy covariance and REA sampling. It indicated good horizontal orientation of the sonic anemometer and that only minor planar-fit corrections were necessary for the vertical wind speed.

The determination of the turbulent CO_2 flux densities from EC measurements was performed with the TK2 software package (*Mauder and Foken*, 2004) and common corrections and quality control measures were applied as outlined by *Ruppert et al.* (2006a) including a WPL-correction for density

---

[1] ^{13}C and ^{18}O isotope ratios in this study refer to the isotope composition of CO_2, i.e. the ratio of $^{13}CO_2$ or $CO^{18}O$ to bulk CO_2. The isotope ratio is expressed in δ-notation. All $\delta^{13}C$ and $\delta^{18}O$ values are reported relative to ^{13}C and ^{18}O isotopic abundances in the international VPDB (Vienna Pee Dee Belemnite) and VPDB-CO_2 standards respectively (CG99 scale, see details in (*Werner et al.*, 2001) and (*Werner and Brand*, 2001)):
$\delta^{13}C=[[(^{13}C/^{12}C)_{sample}-(^{13}C/^{12}C)_{VPDB}]/(^{13}C/^{12}C)_{VPDB}]\cdot 1000$ (‰ VPDB).
$\delta^{18}O=[[(^{18}O/^{16}O)_{sample}-(^{18}O/^{16}O)_{VPDB-CO2}]/(^{18}O/^{16}O)_{VPDB-CO2}]\cdot 1000$ (‰ VPDB-CO_2).

fluctuations (*Webb et al.*, 1980) and a planar-fit rotation (*Wilczak et al.*, 2001) with a vertical wind speed offset correction of 0.032 m.

The problem of axis rotation for REA was raised by *Beverland et al.* (1996b) and *Moncrieff et al.* (1998). We addressed this issue by applying the previously determined planar-fit correction to the vertical wind component online during HREA sampling and were thereby able to correct the vertical wind speed offset. The coordinate rotation of the planar-fit correction (<3°) was applied slightly incorrect to the online data used during HREA sampling. This was due to an unidentified azimuth rotation of 120° between the sonic anemometer raw online data and stored data. However, simulations showed, that this had only minor influence on the updraft and downdraft HREA sample segregation under the conditions of the WALDATEM-2003 experiment. The resulting relative error of the HREA concentration difference due to the erroneous online planar-fit rotation was $-2(\pm3)\%$. This indicates a small underestimation of the concentration difference on average, i.e. slightly reduced efficiency in sampling the maximum concentration difference. This equally applies to the proxy scalar and the scalar of interest. Therefore, the turbulent flux densities will hardly be altered, if they are calculated from measured effective *b*-factors for the proxy scalar like in this study.

In general, the problem of axis rotation and definition of the vertical wind vector for REA and HREA can be addressed. Like described above the planar-fit correction method can be applied as detailed axis rotation procedures for the correction of the vertical wind speed *w* based on fast online analysis of the 3D wind data with a computer. This can be done without time lags from filter functions as asked for by *Moncrieff et al.* (1998) as long as (i) a 3D sonic anemometer is installed long enough before REA sampling to collect a statistically meaningful amount of wind data specific to the site, sonic anemometer and its orientation and (ii) the anemometer orientation remains unchanged for REA sampling. Both criteria can easily be met when REA sampling is performed at sites with permanently installed eddy covariance measurement systems, e.g. at FLUXNET sites.

For the online definition of the hyperbolic deadband during REA sampling according to (4) the vertical wind speed fluctuations *w'* were determined from the 3D wind vector after applying the planar-fit correction. The standard deviation of the vertical wind speed as well as the average and standard deviation of the CO_2 density were continuously recalculated from the most recent 6 min of data applying a linear weighting function by which the newest data was rated three times more important than the oldest data.

3.3. Whole-air REA sampling system and sampling procedure

From close to the measurement path of a sonic anemometer air is sampled through a 1 µm filter and 5 m of Dekabon tubing with polyethylene as inner wall material with a total flow rate of 6.6 L min^{-1}, which assures predominantly turbulent flow (Reynolds number= 2433) in the inlet tube. Plumbing in the system consisted of stainless steel tubing and fittings. All steel and glass material in the system was thoroughly cleaned before assembling by threefold rinsing with Acetone:Hexane 1:1 (nanograde) and subsequent heating. Connection to the REA system and to the glass flasks is made using quick connectors and ultra-torr glass connectors. Viton® only is used as seal material also in membrane pumps and valves. The air stream is splitted into a bypass and a sub-sample of 3 L min^{-1} (Figure 1a). Only the sub-sample is used for REA sampling of updrafts and downdrafts. Constant flow rates ($\sigma \leq 0.5\%$) with minimum pressure drop as asked for by *Bowling et al.* (1998) and *Moncrieff et al.* (1998) are achieved by using low pressure drop flow meters in combination with pulse-width pump motor drivers for the adjustment of constant pump performance, instead of flow controllers. A Nafion® gas-dryer is used for pre-drying of the sample air. Two three-way valves (V1, V2) direct the

sample into the vent (deadband) or the bag 1 or bag 2 reservoirs according to the sign of the vertical wind speed and the size of the deadband (updraft, downdraft). During field experiments the definition of bag 1 and bag 2 as reservoirs for REA updraft or downdraft samples was switched after each sampling interval in order to minimize any systematic influence of one sampling path. A third non-operating valve of the same kind is installed to assure the same flow restriction on all three flow paths. The time lag (7 ms) resulting from the separation of the sampling valves V1 and V2 and the selected flow rate and the valve response times (10-20 ms) are small enough in relation to a desired sampling frequency of 10 Hz (100 ms). In order to allow for larger sample volumes, each bag reservoir consists of two 45 cm diameter Mylar® foil balloons, which are equipped with stainless steel filling tubes, partially perforated, inserted through the foil valve of the balloons and joined with a T-fitting (not shown in Figure 1a and 1b). An airtight seal was achieved by wrapping strong rubber band around the filling tube and foil valve. After REA sampling and before filling into 1 L glass flasks with PCTFE stopcocks the air from the reservoirs is further dried by passing through drying traps filled with magnesium perchlorate granulate ($Mg(ClO_4)_2$). Backpressure valves at the system outlet constantly maintain +500 hPa over ambient pressure in the drying traps and glass flasks in order to minimize potential fractionation by adsorption/desorption processes at the relatively large surfaces of the granulate and flasks.

The dead volume of the bag reservoirs, which cannot be removed by pumping, is about 20 mL. Nevertheless, all old sample in the reservoirs is removed effectively (dilution >>10000:1) prior to REA sampling by flushing the bag reservoirs two times with 10 L of dried air from sampling height through the flushing unit and emptying via the flask-fill units. During a third flushing cycle the bag reservoirs and the two flask-fill units are then conditioned with dried air from sampling height. The bag reservoirs are emptied and conditioning air remains in the drying traps and glass flasks during the next 30-40 min REA sampling procedure. Normally about 10 to 15 L of updraft and downdraft air were collected within 30-40 min of REA sampling with a hyperbolic deadband of H_h=1.0. This allowed flushing the 1 L glass flasks with 6 to 10-fold volume of sample at +500 hPa overpressure. The filling procedure is stopped shortly before one of the bag reservoirs is emptied by closing actuated two-way valves on both sides of the glass flasks and then manually closing the stopcocks of the flasks. Refer to the Table 1 for details on individual system components.
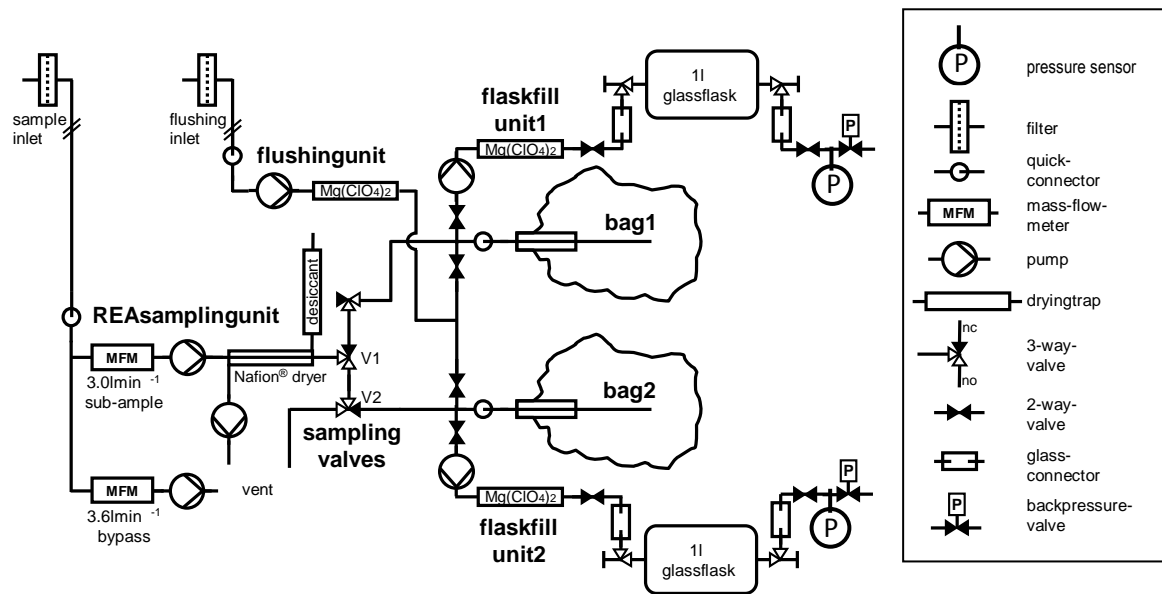
The complete sampling procedure is controlled by the software 'ATEM' (Atmospheric Turbulence Exchange Measurements, (*Ruppert*, 2005)), which allows online monitoring and automated detailed documentation of each sampling procedure. This software also performs the required online analysis of wind and scalar data during REA sampling for the definition of the hyperbolic deadband and corresponding segregation of updraft and downdraft air samples.

3.4. Changes in the whole-air REA sampling system in 2010

In order to avoid overfilling of the balloons larger sample volumes were installed. Two balloons (45 cm diameter) of each up- and downdraft were replaced by one balloon each with 90 cm diameter. Thereby, the volume was enlarged by 28 L to 50 L. Also the risk of leakages in the balloons was reduced, because the well development can be supervised much easier with fewer balloons. In addition to that, balloon holders were constructed that secured an evenly folding of the balloons during filling and well development. The balloon is fixed to a massive circular steel ring - attached to the REA housing - with binder clips and elastic straps that it is always evenly mounted and does not fold. In field experiments the researcher must pay attention to arrange the balloons with the wind direction not to create a sail.

The tube system was checked again for leakages before the project FORKAST in 2010 started. One defect 2-way-valve was replaced by an identical new one. Also the system monitoring was completed by installing a further pressure sensor at glass flask 1. Hence, pressure variabilities can be detected at once and eliminated.
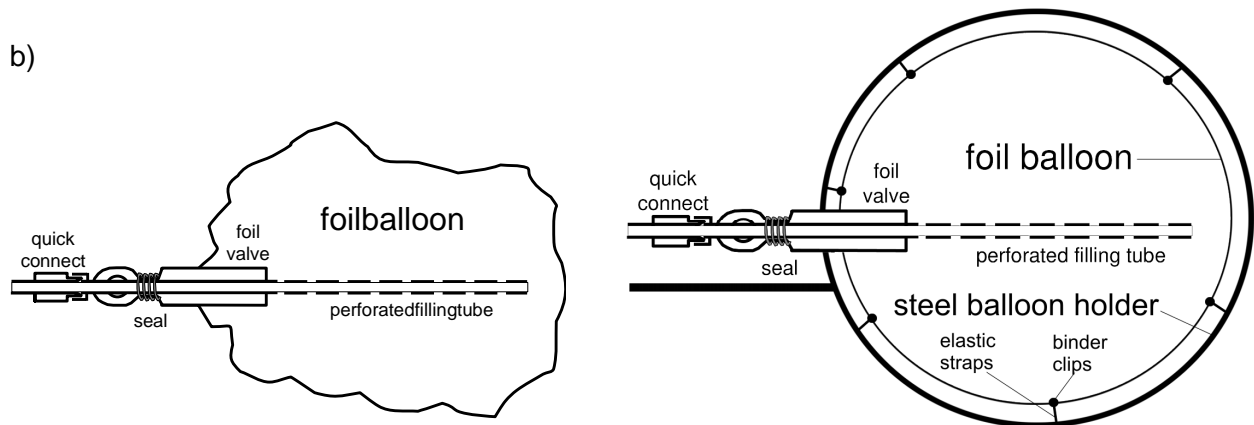
a)

sample inlet

flushing inlet

flushingunit Mg(ClO₄)₂

flaskfill unit1 Mg(ClO₄)₂

1l glassflask

P

P

REAsamplingunit

MFM
3.0lmin⁻¹ sub-ample

desiccant

Nafion® dryer

V1

V2

bag1

sampling valves

MFM
3.6lmin⁻¹ bypass

vent

bag2

Mg(ClO₄)₂

flaskfill unit2

1l glassflask

P

P

P   pressure sensor

filter

quick-connector

MFM   mass-flow-meter

pump

dryingtrap

nc / no   3-way-valve

2-way-valve

glass-connector

P   backpressure-valve

b)

quick connect

seal

foil valve

foilballoon

perforatedfillingtube

quick connect

seal

foil valve

foil balloon

perforated filling tube

steel balloon holder

elastic straps

binder clips

Figure 1. Design of the whole-air REA system (a) for isotope flux measurements with foil balloon bags as intermediate reservoirs (b). The perforated filling tube is inserted into the foil valve of the balloon and tightly sealed with a strong rubber band. The modifications done in 2010 (c) secured an even folding of the balloon and a complete monitoring of the system pressure (a, red circle). Refer to Table 1 and 2 for details on individual components in (a).

Table 1. Whole-air REA System components

Component	Company	Type
Filters	Gelman Sciences Inc., Ann Arbor, MI, USA	ACRO 50, 1.0 µm, Teflon® (PTFE)
Inlet tubing	SERTO jacob GmbH, Fuld-abrück, Germany	SERTOflex-6, 6 mm OD (Dekabon tubing, PE as inner wall material)
Tubing in REA system		Stainless steel, 6 mm OD, cleaned and heated
Connectors	Swagelock, Solon, OH, USA	Stainless steel fittings, quick connects and ultra torr connectors, seals: Viton® (FPM)
Connectors	University of Bayreuth, Germany	Stainless steel fittings, seals: Viton® (FPM)
Mass flow meters (MFM1, MFM2)	Bronkhorst Hi-Tec B. V., Ruurlo, Netherlands	F-111C-HA-33-V, 6 ln/min. (low pressure drop)
Pumps (P1, P3, P4)	KNF Neuberger GmbH, Freiburg, Germany	N 86 AVDC, aluminum, Viton® (FPM)
Pumps (P2 bypass, P5 flushing unit)	KNF Neuberger GmbH, Freiburg, Germany	N 86 KVDC, Ryton®, Viton® (FPM)
Pump (P6 drying air)	FÜRGUT, Aichstetten, Germany	DC24/80S
Pump motor drivers (P1, P2)	Conrad, Hirschau, Germany	192287, pulse-width dc motor driver
Nafion® gas-dryer	Perma Pure Inc., Toms River, NJ, USA	MD-110-48S-4, stainless steel, Nafion® (FPM)
Sampling valves (V1, V2 and dummy)	Bürkert, Ingelfingen, Germany	0330, 3/2 way solenoid valve, 3 mm orifice, stainless steel, Viton® (FPM)
Valves (V3, V4, V5, V6, V7, V8)	Bürkert, Ingelfingen, Germany	6011A, 2/2 way solenoid valve, 2.4 mm orifice, version for analytical applications, stainless steel, Viton® (FPM)
Bag 1, bag 2 (intermediate sample reservoirs)	Anagram International, Inc., Eden Prairie, MN, USA	Mylar® foil balloons, 45 cm, circle shape, (one bag reservoir consists of two balloons which fill with about 14 L each to allow increased sample volumes)
Drying traps	University of Bayreuth, Germany	Magnesium perchlorate granulate, $Mg(ClO_4)_2$, in 200 mm x 20 mm ID glass tubes and glass wool cleaned and heated and Viton® (FPM) seals
Glass flasks	Max-Planck-Institute for Biogeochemistry, Jena, Germany and QVF AG, Ilmenau, Germany	1 L borosilicate glass flasks with PCTFE stopcocks
Pressure sensor (installed at the outlet of one flask filling unit)	Suchy Messtechnik, Lichtenau, Germany	SD-30, -1000…+1500 hPa, stainless steel
Backpressure valves	Riegler & Co. KG, Bad Urach, Germany	Sicherheitsventile DN 8, +500 hPa, brass, Viton® (FPM)

Table 2. Supplemented whole-air REA System components of 2010

Component	Company	Type
Bag 1, bag 2 (intermediate sample reservoirs)	Anagram International, Inc., Eden Prairie, MN, USA	Mylar® foil balloons, 90 cm, circle shape, (now one bag reservoir consists of one bigger balloon which fills with about 50 L each to allow increased sample volumes)
Binder clips	Novus GmbH & Co. KG, Lingen (Ems), Germany	Secure evenly folding, attached to the steel balloon holder by elastic straps
Steel balloon holder	University of Bayreuth, Germany	Fixed with the REA-housing, 1 m diameter, circle shape around each balloon, balloons are connected with binder clips and elastic straps to the holder
Additional pressure sensor (installed at the outlet of the first flask filling unit)	Suchy Messtechnik, Lichtenau, Germany	SD-30, -1000…+1500 hPa, stainless steel

3.5. Synchronization of updraft and downdraft sample segregation

The importance and difficulty of correct synchronization of valve switching in REA and HREA to the vertical wind speed fluctuations under the presence of a unknown time lag as the result of sample flow in a tube is discussed by *Bowling et al.* (1998), *Moncrieff et al.* (1998) and *Fotiadi et al.* (2005). We addressed this problem by performing a differential measurement of sample delay in the tube under defined sampling flow conditions before HREA sampling. The time lag was determined by cross-correlation of vertical wind speed measured at the tube inlet and CO_2 density fluctuations firstly measured at the sample tube inlet and secondly at the segregation valves V1 and V2 (Figure 1a). During HREA sampling, the same defined flow conditions were adjusted and continuously monitored and the time lag measured beforehand was set in the sampling system control software 'ATEM' for valve switching. Thereby we were able to assure correct synchronization of valve switching to the updraft and downdraft events in the turbulence data under defined sampling conditions. The 'ATEM' software also corrected a 200 ms delay of the open-path CO_2 signal due to electronic processing in the instrument. Further details on the synchronization and the online data handling are described by *Ruppert* (2005).

3.6. Whole-air sampling method, density corrections and simulations

In whole-air REA sampling the information on the volume of the sample is preserved, in contrast to sampling on traps. Therefore, the collection of whole-air samples slightly relaxes the demand for very precisely controlled volume flow rates during sampling (*Bowling et al.*, 1998). After passing several meters of tube, updraft and downdraft samples have similar temperature at the pump and segregation valves. No density correction is needed for the measured scalar concentration differences, *b*-factors and turbulent flux densities, because air samples are dried in the sampling process and the updraft and downdraft concentrations in whole-air samples are determined as mixing ratios by laboratory analysis (*Lee*, 2000; *Pattey et al.*, 1992; *Webb et al.*, 1980). Because the whole-air sample collection is not

12

component specific, different non-reactive and stable trace gas components can be analyzed from the same sample.

Relative to sampling on cryo-traps (*Bowling et al.*, 1999a; *Wichura et al.*, 2000), smaller sample volumes are sufficient for whole-air isotope sampling. Smaller sample flow rates, low pressure drop flow meters and the use of flexible Mylar® balloon bags as intermediate storage at ambient pressure minimize pressure changes at orifices in the sampling path and difficulties with fractionation processes (*Bowling et al.*, 1999a). An important practical advantage of whole-air sampling for isotopes compared to cryo-trap sampling is that no liquid nitrogen needs to be carried to and handled in the field.

The system design and operation presented in Section 3.4 was chosen in order to achieve larger whole-air sample volumes compared to the design presented by *Bowling et al.* (2003a) with the aim to increase the sampling accuracy and precision for high precision isotope analysis of $^{13}CO_2$ and $CO^{18}O$. Sufficient amounts of updraft and downdraft air are preserved as dried whole-air samples so that also bulk CO_2, N_2O and CH_4 could be measured. The exact bulk CO_2 mixing ratio of the updraft and downdraft samples is valuable information:

(i)   Both bulk mixing ratio and isotope ratio are required for the determination of the isotope mixing ratio, which forms the basis for the calculation of the turbulent isotope flux density according to (1). With measured bulk CO_2 mixing ratios there is no general need to indirectly infer the mixing ratio from field instrumentation measurements and simulation of the sampling process.

(ii)   Measured effective *b*-factors for CO_2 can be determined according to (2) and from the EC CO_2 flux density. Such *b*-factors integrate all aspects of the sampling process and potential errors. They are compared to *b*-factors from simulation of the ideal HREA sampling process on the CO_2 data record of the EC system in Section 4.3. The comparison of measured effective and simulated *b*-factors forms the basis for the validation of the sampling method and process.

(iii)   The scalar correlation of isotope ratios and bulk CO_2 mixing ratios in updraft and downdraft air samples can be investigated with higher precision. The accumulated updraft and downdraft samples are taken during very short time intervals ranging from 100 ms to several seconds. They therefore represent turbulent exchange processes on relatively short time-scales and can be compared to flask samples collected during longer time intervals. Such data allows investigating the scalar similarity assumptions of the HREA method and the so called EC/flask method (*Bowling et al.*, 1999a; *Bowling et al.*, 2001; *Bowling et al.*, 2003a) on relevant timescales.

For the simulations, the time series of the CO_2 mixing ratio (μ_{CO2}) was determined from the CO_2 density (ρ_{CO2}) record of the open path gas analyzer of the EC system and air density (ρ_a) according to the following equation based on the ideal gas law. Its applicability for simulation studies depending on the design of REA measurement systems is discussed in detail by *Ammann* (1999, p. 92) and *Leuning and Judd* (1996):

$$\mu_{CO2} \equiv \frac{\rho_{CO2}}{\rho_a} = \frac{\rho_{CO2}Tp_0}{\rho_0 T_0 p}\left(1+\mu_{H2O}\right). \qquad (5)$$

Where ρ_0, T_0 and p_0 are respectively the standard dry air density, temperature and pressure. Temperature T was determined from the high frequency sonic anemometers speed of sound measurements and an instrument specific correction for the sonic temperature (*Ruppert et al.*, 2006a). 30 min integrated pressure data from a nearby measurement station were corrected to measurement height in order to yield p. The water vapor mixing ratio (μ_{H2O}) was determined from the high frequency open path gas analyzer H_2O density (ρ_{H2O}) record after application of a similar density correction.

3.7. High precision isotope REA sampling, isotope ratio mass spectrometry (IRMS) and trace gas analysis

High precision sampling for the stable isotopes $^{13}CO_2$ and $CO^{18}O$ of CO_2 requires avoiding sample contamination by fractionation processes. A potential source for isotope sample contamination and fractionation processes are adsorption and desorption effects at large surfaces like the balloon bag reservoirs and the drying traps or related to pressure fluctuations. Such surface effects were reduced by increasing the collected and stored sample volumes and by conditioning bags and flasks before sampling with dried ambient air from sampling height. The flexible balloon bag reservoirs remain at ambient pressure levels. The automation of the conditioning and sample transfer procedures in the new system allowed to assure a constant level of pressure at +500 hPa over ambient pressure in the drying traps and glass flasks, in which the samples are stored until analysis. The automation of the REA system was also intended to improve the measurement repeatability regarding the sampling and filling procedures and to avoid exceptional errors, which might result from manual sample handling. 1 L glass flasks with PCTFE stopcocks are used for sample storage and transport into the laboratory. The large sample volume and sampling flask conditioning with dry air are required for subsequent high precision isotope and trace gas analysis (*Brand*, 2005; *Rothe et al.*, 2005; *Sturm et al.*, 2004; *Werner et al.*, 2001).

For isotope analysis, sample air from the flasks is directed into a home made trapping line ('BGC AirFlo', (*Werner et al.*, 2001) attached to a MAT 252 isotope ratio mass spectrometer (IRMS) system. The air is pumped through the cryogenic trapping system and CO_2 is frozen out at a temperature of – 196 °C using a flow of 60 bml/min. The dual inlet system of the MAT 252 is used as the pumping infrastructure. Sample CO_2 is extracted from 600 mL of air and, after pumping away residual air and allowing for complete isotopic equilibration, measured directly from the sampling reservoir via the 252 changeover valve. The system is under full computer control for reliable timing and unattended operation. The isotopic analysis is performed with high level of overall precision for both $\delta^{13}C$ and $\delta^{18}O$ at about 0.013‰ vs. VPDB and 0.02% vs. VPDB-CO_2 respectively. For further details on the IRMS high precision analysis system and procedures see *Werner et al.* (2001).

The CO_2, N_2O and CH_4 mixing ratios were determined in the trace gas laboratory of the Max-Planck Institute in Jena, Germany. A chromatographic run starts with flushing sample gas from the pressurized glass flask through the two sample loops. The amount of gas is controlled by a mass flow controller. For some samples lacking pressure above ambient in the glass flask a manual injection method with a syringe was applied. The lack of pressure in these glass flasks was due to a temporal malfunctioning of a backpressure valve during the filling procedure. After equilibration with ambient pressure the loop gases were injected onto the respective precolumn using Valco 10 port injection valves. After the analytes have passed the precolumn and entered the main GC-column the Valco 10 port valves are switched again to backflush the precolumns. Injections are made alternating between sample gas and one reference gas ("working standard"). The ratio of a sample analysis and the mean of the two bracketing working standard analysis are calculated for quantification. With this approach, average relative

precisions of 0.02 % for CO_2 (0.08 µmol mol^{-1} at atmospheric mixing ratio levels), 0.04% for N_2O (0.13 nmol mol^{-1}) and 0.07% for CH_4 (1.3 nmol mol^{-1}) are achieved. The calibration scale for each compound is set using standard gases calibrated by the Central Calibration Laboratory (CMDL, Boulder, Colorado) as required by the World Meteorological Organization (WMO) and in compliance with recommendations of the eleventh WMO/IAEA CO_2 Experts Meeting on the CO_2 calibration scale for measurements of atmospheric samples (direct link to the WMO mole fraction scale, see recommendations in the reports by *Jordan and Brand* (2003) and *Miller* (2006)).

3.8. Field experiments

The whole-air REA system was used to collect updraft and downdraft air during the field experiment WALDATEM-2003 (Wavelet Detection and Atmospheric Turbulent Exchange Measurements 2003, *Thomas et al.*, 2004). Samples were collected above a spruce forest (*Picea abies, L.*) with a plant area index (PAI) of 5.2 m^2 m^{-2} (*Thomas and Foken*, 2007) and an average canopy height of 19 m. The experiment site Waldstein/Weidenbrunnen (GE1-Wei) is part of the FLUXNET network and is located in the Fichtelgebirge mountains in Germany (50°08'31" N, 11°52'01" E, 775 m a.s.l.) on a slope of 2°. A detailed description of the site can be found in *Gerstberger et al.* (2004) and *Staudt and Foken* (2007). A sonic anemometer (R3-50, Gill Instruments Ltd., Lymington, UK) and an open path CO_2 and H_2O analyzer (LI-7500) are installed on a tower at 33 m and their data is used for continuous EC measurements at the site. During the WALDATEM-2003 experiment, the EC data was used also for the HREA measurements with the whole-air REA system. The sample inlet was installed at 33 m just below the sonic anemometer and samples were directed through a Teflon® filter into the whole-air REA system as described in Section 3.3. The whole-air REA system was positioned on the tower at a platform at 28 m. Automated sample transfer procedures were used to immediately store the samples in the glass flasks and avoid uncontrolled pressure changes and any contamination in the field.

In 2010 the whole-air REA system was checked and reactivated for the subproject 5 of the joint research project FORKAST (Investigation of carbon fluxes on grasslands in Northern Bavarian low mountain ranges under extreme climate conditions). The experiment was conducted on a submontane grassland site at the edge of the low mountain range "Fichtelgebirge", 624 m a.s.l. (50°05'25''N, 11°51'25''E) in northeast Bavaria, Germany. For the last 10 years the experimental site was only used as extensively managed grassland without fertilization or grazing, but sporadic mowing, 1 or 2 times a year. North of the study site the "Großer Waldstein" with 877 m and south the "Schneeberg" with 1051 m elevation are located. These two mountains generate a channeled wind field on the site with East and first of all West as dominating wind directions (prevailing wind direction 263°). Also in this experiment the REA-measurements were accompanied by continuous EC measurements. Therefore, a 3D sonic anemometer (CSAT3, Campbell Scientific, Inc., Logan, Utah USA) and an open path CO_2 and H_2O analyzer (LI-7500, LI-COR Biosciences, Lincoln, Nebraska USA) were installed 2.5 m above ground. The EC data was again used for the HREA measurements. The sample inlet was installed in 2.5 m height, close to the middle of the measurement path of the conic anemometer. The whole-air REA system was positioned perpendicular to the main wind direction. Due to the already mentioned channeled wind field disturbances of the measurements could be avoided. In the FORKAST experiment also isotopic pulse labeling of the ecosystem with the stable isotope ^{13}C was performed. Thereby carbon fluxes though the ecosystem can be investigated. The whole-air REA measurements served the purpose to evaluate the influences of the natural abundance ^{13}C fluxes in the atmosphere on those tracer experiments.

4. Results and Discussion

4.1. Foil balloon bag tests

   The importance of the material selection and treatment for air sample isotope analysis is highlighted by tests results presented by *Schauer et al.* (2003) in which heated stainless steel tubing, Viton® seals and polyethylene (PE) were found not to contaminate CO_2 isotope samples. The isotopic integrity regarding $\delta^{13}C$ of whole-air samples during storage of up to 60 min in Mylar® foil balloon bags with PE as inner wall material was demonstrated by *Bowling et al.* (2003a). However, a bias was found for residence times longer than 60 min and for $\delta^{18}O$. We therefore performed similar tests with the same kind of foil balloon bags. Air sampled from one pressurized air tank was analyzed after varying residence time in the balloon bags by high precision IRMS. A first test with brand new balloons flushed three times with air from the tank showed significant contamination of the air samples with heavier isotopes (Figure 2) depending on time after flushing. The contamination presumably is the result of the release of substances with fossil origin from the balloon inner wall material PE.

   For a second test, we treated the balloons by flushing them for about 4 days with nitrogen and dried air and by exposing them to intense direct sunlight. Afterwards, 9 balloon bags were first filled and emptied three times in the morning of the second test and then filled consecutively with air form a tank during the day, allowing different sample residence times up to 2 h before analysis. Only after the treatment, the balloon bags lacked signs of significant contamination (Figure 3, (WALDATEM-2003 (a) and (b), FORKAST-2010 (c). The standard deviation for both $\delta^{13}C$ and $\delta^{18}O$ isotope ratios from the 9 samples were acceptably low and the average value of the balloon bag samples compared well with an air sample taken directly from the tank and stored in a glass flask. These results demonstrate the general suitability of foil balloon bags for both ^{13}C and [18]O isotope air sampling and intermediate storage, which is normally restricted to 30-40 min in REA.
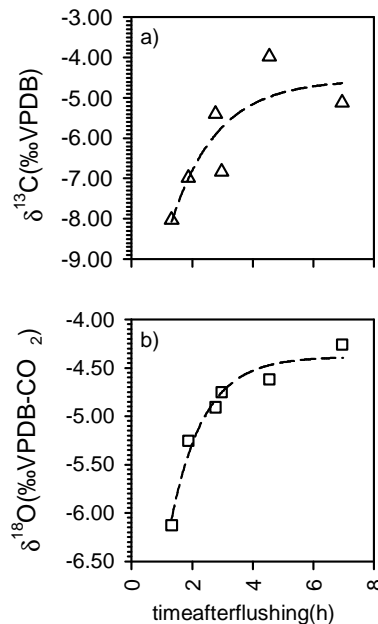

Figure 2. Foil balloon bag test for [13]C (a) and [18]O (b) isotope sampling before cleaning. The symbols represent the measured isotope ratios in 6 individual balloon bags. Each bag was flushed 3 times with sample air from one air tank on its first usage. Dashed lines indicate the progressive contamination of the air with heavier isotopes after the flushing procedure.
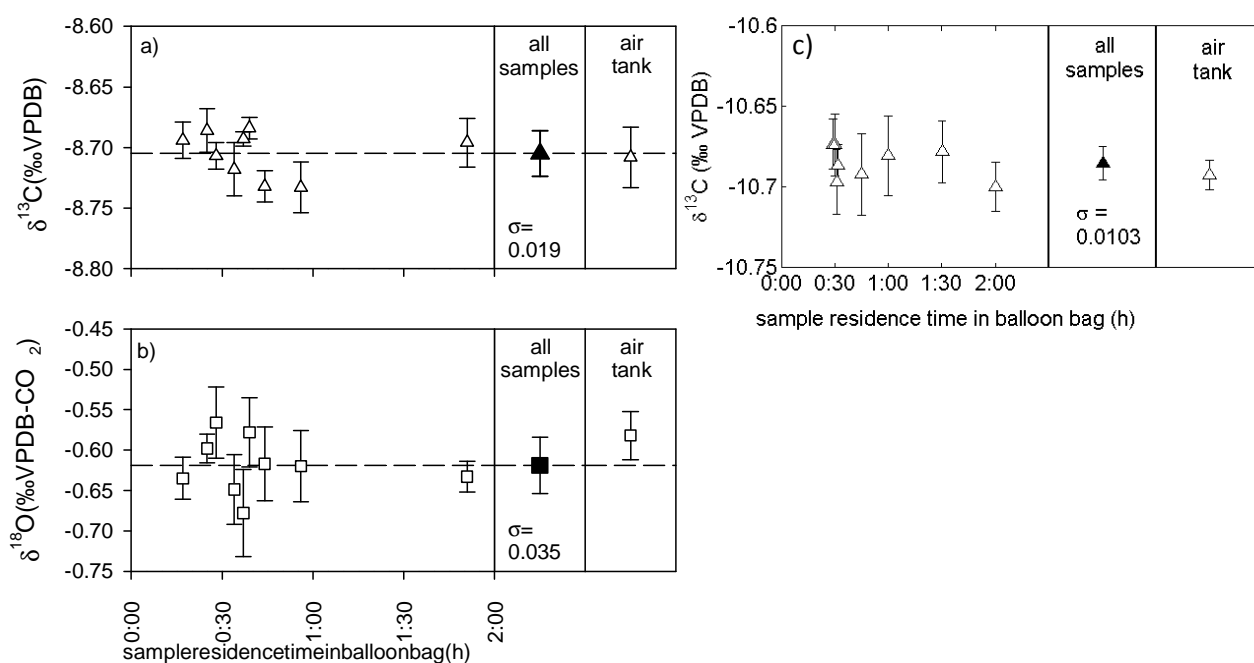
16

Figure 3. Foil balloon bag test for ^{13}C (a) and ^{18}O (b) isotope sampling after bag cleaning (WALDATEM-2003 (a) and (b), FORKAST-2010 (c). Symbols in the leftmost section of the figure represent isotope ratios measured in air sampled from one tank after different residence times in 9 different balloon bags. Error bars indicate the standard deviation of up to 12 repeated measurements on the same air sample, which form the basis for the specification of its isotope ratio with high precision. Dashed lines and the solid symbol in the right section of the figure represent the average isotope ratio measured in the 9 balloon bags. The corresponding error bar indicates the standard deviation of the 9 specified isotope ratios from the balloon bag samples. As reference, the rightmost section of the figure shows the isotopic ratio of air sampled from the air tank into a glass flask without residence in a balloon bag. Note the difference in scales when comparing to Figure 2.

4.2. Whole-air REA system tests

We repeated the tests with the complete whole-air REA system described in Section 3. Beforehand, small leaks in the REA system were located by performing leak tests with high-vacuum and removed. In a third test for isotopic integrity (no figure), samples were directed through different parts of the system (REA sampling unit, flushing unit, flask fill unit, see Figure 1a). Small standard deviations of $\delta^{13}C$ (0.022‰) and $\delta^{18}O$ (0.021‰) isotopic ratios in 15 samples assured, that the surfaces of other materials in the system which contact the sample (glass, stainless steel, aluminum, Viton® seals, Nafion®, $Mg(ClO_4)_2$ granulate) were clean and no source of sample contamination.

In a fourth test we operated the complete whole-air REA system in the same way as for field sampling with automated sampling procedures after threefold flushing of the balloon bags, drying traps and glass flasks (see Section 3.3) but by drawing sample air and air for flushing and conditioning from a tank. The samples were stored for about 30 min in the balloon bags and filled into glass flasks for later analysis. The standard deviation of $\delta^{13}C$ (0.014‰) and $\delta^{18}O$ (0.019‰) in 19 samples were close to the measurement precision of the mass spectrometer and the average isotopic ratios matched well with an air sample from the tank stored in a glass flask (Figure 4).

Before producing the sample J585, the complete REA system, balloon bags and glass flasks were contaminated with room air (dotted line), which presumably had isotopic ratios depleted by human

17

breath compared to the pressurized air tank. The isotopic ratios of samples produced afterwards show no systematic deviation from the average, which indicates, that the threefold flushing procedure is effective in removing old sample air.

The test results with the treated balloon bags (9 samples) and the complete whole-air REA system with the automated field sampling procedure (19 samples) demonstrate the isotopic integrity of samples taken with the system and the systems suitability for high precision isotope sampling. Nevertheless, the sample air residence time in the balloon bags should be restricted to the minimum needed for REA sampling (30-40 min) and the samples should then be transferred to glass flasks for the transport from the field to the laboratory.

The whole air REA system test in 2010 was accomplished in a similar way. The contamination with room air in the beginning of the test becomes visible in the J1 samples by slightly higher $\delta^{13}C$ values (Figure 4c). The normalization of the values J2 (and all following values) proofs, that the system is no longer contaminated after only one flushing process.
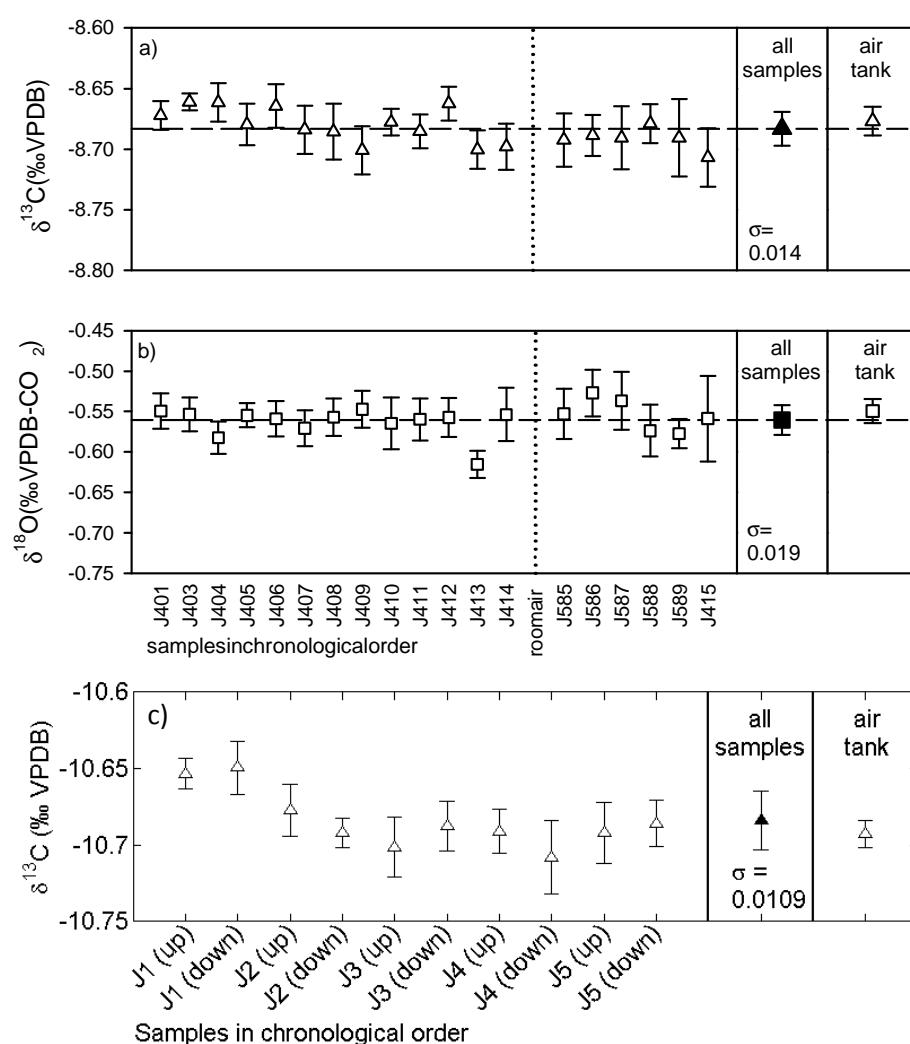

Figure 4. Test of the complete whole-air REA system for ^{13}C (a) and ^{18}O (b) isotope sampling cleaning (a) and (b) WAL-DATEM-2003, (c) FORKAST-2010). The usage of the symbols and lines follows the logic of Figure 3. Air from the tank was used for threefold flushing and directed through the REA sampling system, stored in the balloon bags and sampled into glass flasks in the same manner as required for REA sampling in the field. Subsequently, the ^{13}C and ^{18}O isotope ratios of CO_2 sampled into the glass flasks were measured.

18

4.3. HREA simulation and b-factors

In order to check the efficiency of the updraft and downdraft sample segregation HREA sampling was simulated for each sampling interval using the actual valve switching record from the field experiments to segregate and virtually accumulate updraft and downdraft samples of the μ_{CO2} time series determined by (5).

The simulated average updraft and downdraft mixing ratios are compared to average updraft and downdraft CO_2 mixing ratios measured in the whole-air samples in Figure 5. The least square linear regression for updraft and downdraft samples is well defined (R^2=0.93) and results in a slope very close to one. This is a proof for correct instrument performance regarding the HREA sample segregation and accumulation process. The average offset of the measured values of +0.26 µmol mol^{-1} indicates good calibration of field instruments.
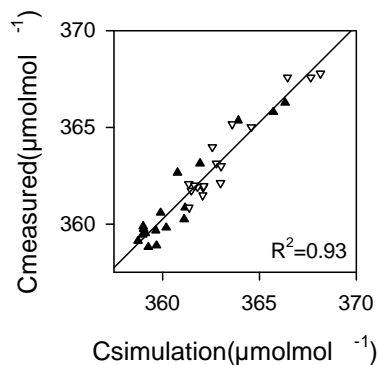

Figure 5. Measured updraft and downdraft CO_2 mixing ratios in HREA whole-air samples plotted against CO_2 mixing ratios from simulation of HREA sampling based on the EC CO_2 time series (updraft solid and downdraft unfilled triangles) with their least square linear regression (line).

Effective b-factors were determined from the measured updraft and downdraft CO_2 mixing ratio difference $\overline{c}_\uparrow - \overline{c}_\downarrow$ and the turbulent CO_2 flux density measured by EC according to (2). The effective b-factors can be compared to b-factors derived from the simulated mixing ratio differences (Figure 6). The simulated b-factors are very sensitive to the applied density correction (5), because of small mixing ratio differences relative to the absolute values of the mixing ratio. Simulations with simplified density corrections for the CO_2 mixing ratio data resulted in significant mismatches between the measured and simulated updraft and downdraft absolute CO_2 mixing ratios and consequently less correlation between measured and simulated b-factors.

Both measured and simulated values of the b-factors show the variability that must be expected for HREA as well as for REA from the skewness in the JFD of the vertical wind speed and the scalar and from sampling effects which depend on the eddy reversal frequency (*Baker et al.*, 1992). Like in other studies, which compare measured effective b-factors to simulated b-factors (*Baker et al.*, 1992; *Beverland et al.*, 1996b; *McInnes et al.*, 1998), we find, that simulated values tend to underestimate measured values especially at higher b-factors. High b-factors were related to high turbulent flux density (R^2=0.42) and reduced sampling efficiency, (R^2=0.78), i.e. sampled concentration difference per turbulent flux density. The observed underestimation is the result of some inefficiency of the physical sampling process in separating updraft and downdraft samples compared to the virtual 'digital' sampling in HREA simulations (*Baker et al.*, 1992; *Beverland et al.*, 1996b; *Lenschow and Raupach*, 1991;

19

Massman, 1991; *McInnes et al.*, 1998; *Moncrieff et al.*, 1998). Measured effective *b*-factors resulting from the real physical sampling process integrate such deficiencies. In order to calculate REA turbulent flux densities from measured concentration differences by (1), measured effective *b*-factors should therefore be preferred in comparison to simulated *b*-factors.

Virtual sampling results in a slightly higher concentration differences and consequently lower simulated *b*-factors according to (2). Simulated *b*-factors therefore require validation when used to replace effective *b*-factors that could not be measured, and an instrument and experiment specific correction needs to be found (*Beverland et al.*, 1996a; *McInnes et al.*, 1998), e.g. based on a least square linear regression function like shown in Figure 6. The overestimation of concentration differences from virtual 'digital' sampling of a proxy scalar in REA simulations evaluated for the *b*-factors without correction according to (2) can cause systematic underestimation of flux densities according to (1).

The size of the residuals of the measured *b*-factors in Figure 6, quantified with 0.03 by the corresponding standard error, related to their range of absolute values of 0.15 to 0.35 provides an estimate of the average uncertainty of CO_2 fluxes measured by HREA with a hyperbolic deadband of H_h=1.0 of about 10 to 20%. This quantifies the measurement uncertainty of the sampling system and method in reference to EC flux measurements for a component for which sufficient analytical precision is available during sample analysis (signal/noise ratio >10, Section 4.4).
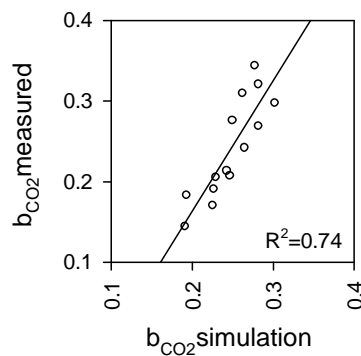

Figure 6. Effective *b*-factors derived from measured CO_2 mixing ratios in HREA whole-air samples in relation to simulated *b*-factors (circles) and their least square linear regression (line).

More information about HREA simulations and *b*-factors, i.e. diurnal cycles of *b*, determined with various proxy scalars, is presented by Hübner (2010). There also the effects of potentially wrong *b*-factors on the REA-flux were evaluated.

4.4. Maximum concentration difference by HREA for isotope analysis

The application of REA with hyperbolic deadbands, i.e. the HREA method (*Bowling et al.*, 1999b), is intended to maximize the concentration difference of the scalar of interest, so that it can be resolved with sufficient precision by laboratory analysis. Simulations of REA (H_w=0.6) and HREA (H_h=1.0) with the WALDATEM-2003 data showed a concentration difference increase by a factor of 1.78 (Table 2), which is comparable to the factor of 1.84 derived from results presented by *Bowling et al.* (1999b). The factor reduces to 1.73 for the WALDATEM-2003 data or 1.65 in the work of *Ruppert et al.* (2006b), if imperfect scalar similarity between the scalar of interest and the proxy scalar is considered. However, all factors reported above are the result of simulations with an ideal definition of the hyperbolic deadband based on scalar data from the complete sampling interval (lines in Figure 7).
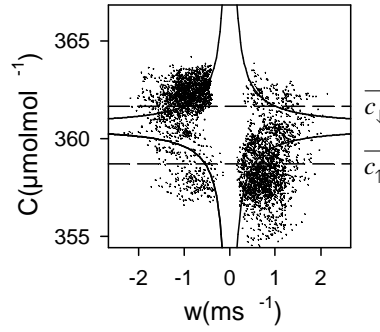
Figure 7. Plot of the effective hyperbolic sample selection for a 30 min sampling interval (dots) regarding vertical wind speed w and the open path CO_2 mixing ratio data C from the WALDATEM-2003 experiment, day of the year 188, 12:00-12:30. The sample selection is based on the original HREA valve switching record. Both axes are scaled to the 30 min average ± 4 standard deviations. The solid lines indicate the ideal hyperbolic deadband with the size $H_h=1.0$ in respect to the 30 min statistics. The dashed lines indicate the average CO_2 mixing ratios of updraft ($\overline{c}_\uparrow$: $w>0$) and downdraft ($\overline{c}_\downarrow$: $w<0$) air samples, resulting from the effective hyperbolic sample selection.

During the real sampling process, only historic scalar data is available. The mean scalar value is defined based on a filter function and the center of the hyperbolic deadband moves up and down along the scalar axis. This leads to less rigorous rejection of samples with average scalar values (see dots close to the center of Figure 7). Consequently, the average scalar concentration difference between updrafts and downdrafts is slightly decreased, e.g. the CO_2 mixing ratio difference $\overline{c}_\uparrow - \overline{c}_\downarrow$ in Figure 7. The application of a wind-deadband (REA) instead of a hyperbolic deadband (HREA) would incorporate even more air with average CO_2 mixing ratios (e.g. around 360 µmol mol^{-1} in Figure 7) in updraft and downdraft air samples and thereby further decrease the mixing ratio difference. Simulations based on the recorded valve switching from the WALDATEM-2003 experiment showed, that the realistic concentration difference increase between REA ($H_w=0.6$) and HREA ($H_h=1.0$) is only 1.63 (Table 2). The corresponding expected CO_2 mixing ratio difference from HREA simulations based on the effective sample segregation during the experiment with a hyperbolic deadband of $H_h=1.0$ is $2.4(\pm0.5)$ µmol mol^{-1}. The observed mixing ratio differences were only slightly smaller, $(2.3(\pm0.6)$ µmol mol^{-1}, Table 2, Figure 8a), reflecting also the physical air sampling effects discussed in Section 4.4. However, these also affect REA sampling with a wind-deadband and an effective relative concentration difference increase close to 1.63 can be assumed.
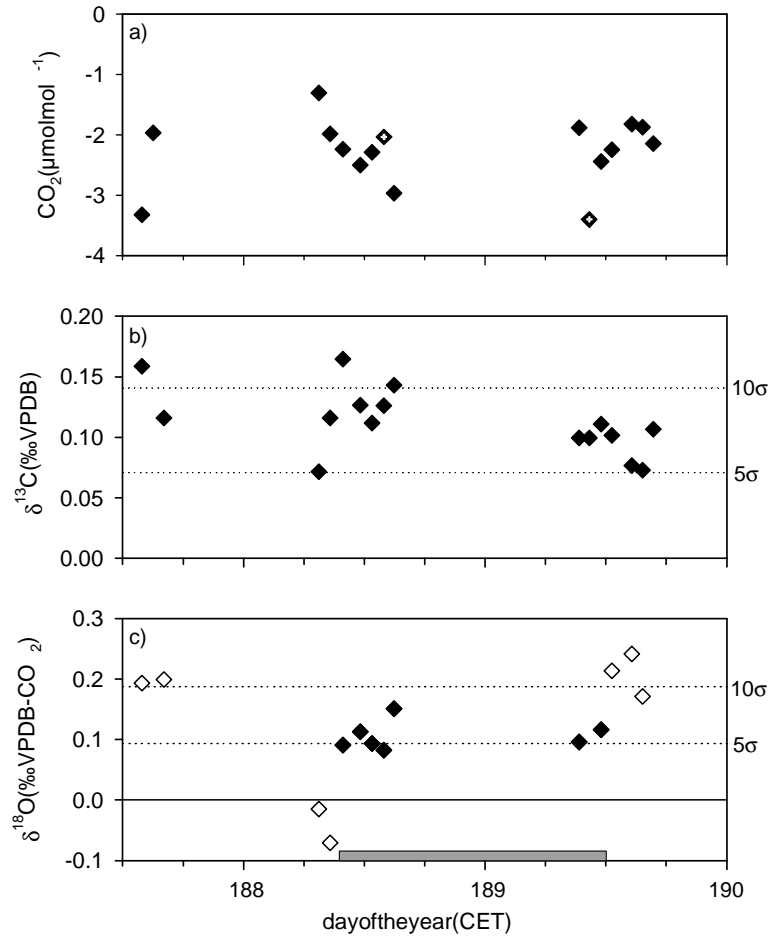
21

Figure 8. CO_2 mixing ratio differences (a) and ^{13}C (b) and ^{18}O (c) isotope ratio differences in updraft and downdraft REA air samples (solid diamonds). ^{18}O isotope ratio differences presumably influenced by incomplete drying out of the period marked with a gray bar are indicated as unfilled diamonds. Dotted lines indicate the fivefold and tenfold standard deviations specified in Section 4.2 and Figure 4 in order to assess the measurement precision for the isotope samples.

We avoided increasing the hyperbolic deadband size H_h further, because in contrast to results of ideal simulations, no significant additional concentration difference increase could be expected with larger hyperbolic deadbands when acknowledging the realistic sampling process. Also, the representativeness of updraft and downdraft samples for the JFD would be further decreased if larger deadbands would be applied.

During the WALDATEM-2003 experiment, the overall proportions of evaluated samples in each sampling interval were 14.7($\pm$3.0)% updrafts and 9.1($\pm$2.6)% downdrafts. The difference in the number of updraft and downdraft samples results from skewness in the JFD and was discussed by *Bowling et al.* (1999b). The authors suggest an optimum deadband size at H_h=1.1 and an asymmetric adjustment of the hyperbolas. We decided not to adjust the symmetric shape of the hyperbolic deadband, in order to prevent artifacts that could result from changing shapes of the JFD, which have to be considered above tall vegetation.

CO_2 mixing ratio differences of whole-air HREA updraft and downdraft samples in the range of –1.3 to –3.9 µmol mol^{-1} exceeded the tenfold measurement precision. Two samples marked with a '+' in Figure 5a showed relatively small sample proportions. Their representativeness in respect to the JFD remains questionable. Furthermore, reduced precision of the CO_2 mixing ratio difference can

result from the transfer of relatively small amounts of sample air. Therefore, only simulated and corrected b-factors were used for the estimation of the isotope fluxes of these two samples in Figure 8b and 8c.

The ^{13}C and [18]O isotopic differences, i.e. the difference of the isotope ratios of updraft and downdraft air samples, observed by the HREA measurements during WALDATEM-2003 were on average 0.11($\pm$0.03)‰ for δ^{13}C and 0.11($\pm$0.02)‰ for δ^{18}O during the time with sufficient sample drying (Table 2). Most values lie between the fivefold and tenfold standard deviations found in the whole-air REA system tests (dashed lines in Figure 8b and 8c, compare Figure 4). Similar δ^{13}C differences were reported for many samples by *Bowling et al.* (1999a). Nevertheless, the small differences of the isotope ratios ask for high precision in the sample analysis. Based on the comparison of the isotopic differences and the precision determined in the whole-air REA system tests a measurement uncertainty due to the resolution of the isotopic differences of 10% to 20% can be estimated.

The mixing ratio differences observed for CH_4 and N_2O in daytime samples taken above the spruce forest at Waldstein/Weidenbrunnen during the WALDATEM-2003 experiment ranged from -2.9 to 1.6 nmol mol^{-1} for CH_4 and -0.37 to 0.49 nmol mol^{-1} for N_2O. Most mixing ratio differences were in the order of measurement precision (1.3 nmol mol^{-1} for CH_4 and 0.13 nmol mol^{-1} for N_2O) and consequently too small to be resolved by HREA sampling and whole-air analysis without pre-concentration on a trap. The indication of negative concentration differences and downward direction of CH_4 and N_2O fluxes on average of the daytime samples was not significant (Table 2).

Table 2. Concentration difference increase achieved by HREA sampling during the WALDATEM-2003 experiment and comparable data.

Scenario	Concentration difference increase HREA (H_h=1.0) / REA (H_w=0.6)	Average scalar concentration differences HREA (H_h=1.0)
Simulation, ideal	1.78 this study, 1.84 (*Bowling et al.*, 1999b)	CO_2: 4.9($\pm$2.4) µmol mol^{-1} (*Bowling et al.*, 1999b) based on data from Eastern USA deciduous forest
Simulation, imperfect scalar similarity	1.73 this study, 1.65 (*Ruppert et al.*, 2006b)	
Simulation, proxy scalar and σ_w statistics defined from previous data and filter function	1.63 this study	CO_2: 2.4($\pm$0.5) µmol mol^{-1} this study
Measured, including physical sampling effects		CO_2: 2.3($\pm$0.6) µmol mol^{-1} δ^{13}C: 0.11($\pm$0.03) ‰ VPDB δ^{18}O: 0.11($\pm$0.02) ‰ VPDB-CO_2 CH_4: -0.4($\pm$1.2) nmol mol^{-1} N_2O: -0.02($\pm$0.26) nmol mol^{-1}

5. Conclusion

Lab experiments with foil balloon bags and the complete whole-air REA system demonstrate their suitability for high precision isotope sampling for both ^{13}C and ^{18}O isotopes of CO_2. This was indicated by a close match of isotope ratios found in air samples from two independent sampling systems. We therefore conclude that foil balloons are suitable flexible air collection containers for intermediate storage after cleaning as described in Section 4.1. Large whole-air sample volumes, precise flow and pressure control, careful material selection and treatment and effective sample drying helped to increase the sampling accuracy of the complete whole-air REA system especially for ^{18}O isotopes.

$\delta^{13}C/CO_2$ and also $\delta^{18}O/CO_2$ correlations can therefore readily be investigated even at relatively small ranges of CO_2 mixing ratios.

HREA measurements provide additional information on the scalar variation and on the most significant events in the turbulent isotopic exchange above the ecosystem for the determination of isofluxes.

The comparison of measurement results and simulations of HREA sampling for bulk CO_2 confirmed good instrument performance and indicated 10 to 20% uncertainty for the quantification of fluxes due to the sampling method. The measured effective *b*-factors should be preferred for flux determination. Simulated *b*-factors require validation and potentially correction in order to prevent the risk of systematic underestimation of fluxes. Detailed axis rotation procedures for REA and HREA sampling without a time lag (*Beverland et al.*, 1996b; *McInnes et al.*, 1998; *Moncrieff et al.*, 1998) can be implemented by evaluating the 3D wind vector and performing online planar-fit corrections (*Wilczak et al.*, 2001). The precise synchronization of REA segregation valve switching can be achieved under defined sample flow conditions by differential cross-correlation measurements as outlined in Section 3.4. A concentration difference increase of 63% was achieved by applying the HREA sampling method instead of classical REA. Nevertheless, relatively small isotopic differences in updraft and downdraft samples collected during the WALDATEM-2003 and FORKAST-2010 experiments required high precision isotope analysis. The measurement uncertainty due to the chemical resolution of the isotope ratio differences was estimated at 10 to 20%.

Whole-air HREA in combination with high precision isotope analysis can quantify isofluxes of $^{13}CO_2$ and $CO^{18}O$ and collect additional information on the scalar correlation to bulk CO_2, representing the relatively short timescale of up- and downdrafts in the turbulent exchange above an ecosystem.

6. Acknowledgments

References

Ammann, C. (1999), *On the applicability of relaxed eddy accumulation and common methods for measuring trace gas fluxes*, Geographisches Institut der ETH Zürich ed., ETH Zürich, Zürich, 230 pp.

Ammann, C., and F. X. Meixner (2002), Stability dependence of the relaxed eddy accumulation coefficient for various scalar quantities, *J. Geophys. Res., 107*, (D8), 4071, doi:10.1029/2001JD000649.

Baker, J. M., J. M. Norman, and W. L. Bland (1992), Field-scale application of flux measurement by conditional sampling, *Agric. For. Meteorol., 62*, 31-52.

Beverland, I. J., J. B. Moncrieff, D. H. O'Neill, K. J. Hargreaves, and R. Milne (1996a), Measurements of methane and carbon dioxide fluxes from peatland ecosystems by the conditional-sampling technique, *Quart. J. Roy. Meteor. Soc., 122*, 819-838.

Beverland, I. J., D. H. Oneill, S. L. Scott, and J. B. Moncrieff (1996b), Design, construction and operation of flux measurement systems using the conditional sampling technique, *Atmos. Environ., 30*, 3209-3220.

Bowling, D. R., A. A. Turnipseed, A. C. Delany, D. D. Baldocchi, J. P. Greenberg, and R. K. Monson (1998), The use of relaxed eddy accumulation to measure biosphere-atmosphere exchange of isoprene and other biological trace gases, *Oecologia, 116*, 306-315.

Bowling, D. R., D. D. Baldocchi, and R. K. Monson (1999a), Dynamics of isotopic exchange of carbon dioxide in a Tennessee deciduous forest, *Glob. Biogeochem. Cycles, 13*, 903-922.

Bowling, D. R., A. C. Delany, A. A. Turnipseed, D. D. Baldocchi, and R. K. Monson (1999b), Modification of the relaxed eddy accumulation technique to maximize measured scalar mixing ratio differences in updrafts and downdrafts, *J. Geophys. Res., 104*, (D8), 9121-9133.

Bowling, D. R., P. P. Tans, and R. K. Monson (2001), Partitioning net ecosystem carbon exchange with isotopic fluxes of CO_2, *Global Change Biol., 7*, 127-145.

Bowling, D. R., D. E. Pataki, and J. R. Ehleringer (2003a), Critical evaluation of micrometeorological methods for measuring ecosystem-atmosphere isotopic exchange of CO_2, *Agric. For. Meteorol., 116*, 159-179.

Bowling, D. R., S. D. Sargent, B. D. Tanner, and J. R. Ehleringer (2003b), Tunable diode laser absorption spectroscopy for stable isotope sudies of ecosystem-atmosphere CO_2 exchange, *Agric. For. Meteorol., 118*, 1-19.

Brand, W. A. (2005), O_2/N_2 Storage Aspects and Open Split Mass Spectrometric Determination, in *Proceedings of the 12th WMO/IAEA Meeting of Expert on Carbon Dioxide Concentration and Related Tracers Measurements Techniques, Toronto, Canada, Sept. 2003, WMO-GAW Report 161*, edited by D. Worthy and L. Huang, pp. 146-151.

Businger, J. A., and A. C. Delany (1990), Chemical sensor resolution required for measuring surface fluxes by three common micrometeorological techniques, *J. Atmos. Chem., 10*, 399-410.

Businger, J. A., and S. P. Oncley (1990), Flux Measurement with conditional sampling, *J. Atmos. Ocean. Tech., 7*, 349-352.

Canadell, J. G., H. A. Mooney, D. D. Baldocchi, J. A. Berry, J. R. Ehleringer, C. B. Field, S. T. Gower, D. Y. Hollinger, J. E. Hunt, R. B. Jackson, S. W. Running, G. R. Shaver, W. Steffen, S. E. Trumbore, R. Valentini, and B. Y. Bond (2000), Carbon metabolism of the terrestrial biosphere: A multitechnique approach for improved understanding, *Ecosystems, 3*, 115-130.

Delany, A. C., S. P. Oncley, J. A. Businger, and E. Sievering (1991), Adapting the conditional sampling concept for a range of different chemical species, paper presented at Seventh symposium on meteorological observations and instruments, American Meteorological Society, Boston, New Orleans, La., 14-18 January 1991.

Desjardins, R. L. (1977), Description and evaluation of a sensible heat flux detector, *Boundary-Layer Meteorol., 11*, 147-154.

Ehleringer, J. R., D. R. Bowling, L. B. Flanagan, J. Fessenden, B. Helliker, L. A. Martinelli, and J. P. Ometto (2002), Stable isotopes and carbon cycle processes in forests and grasslands, *Plant Biology, 4*, 181-189.

Foken, T., R. Dlugi, and G. Kramm (1995), On the determination of dry deposition and emission of gaseous compounds at the biosphere-atmosphere interface, *Meteorol. Z., 4*, 91-118.

Foken, T., M. Göckede, M. Mauder, L. Mahrt, B. Amiro, and W. Munger (2004a), Post-field data qualtiy control, in *Handbook of Micrometeorology*, edited by X. Lee, et al., pp. 181-208, Kluwer, Dordrecht.

Fotiadi, A. K., F. Lohou, A. Druilhet, D. Serca, Y. Brunet, and R. Delmas (2005), Methodological development of the conditional sampling method. Part I: Sensitivity to statistical and technical characteristics, *Boundary-Layer Meteorol., 114*, 615-640.

Gao, W. (1995), The vertical change of coefficient b, used in the relaxed eddy accumulation method for flux measurement above and within a forest canopy, *Atmos. Environ., 29*, 2339-2347.

Gerstberger, P., T. Foken, and K. Kalbitz (2004), The Lehstenbach and Steinkreuz Catchments in NE Bavaria, Germany, in *Biogeochemistry of Forested Catchments in a Changing Environment: A German case study*, edited by E. Matzner, pp. 15-41, Springer, Berlin.

Guenther, A., W. Baugh, K. Davis, G. Hampton, P. Harley, L. Klinger, L. Vierling, P. Zimmerman, E. Allwine, S. Dilts, B. Lamb, H. Westberg, D. Baldocchi, G. Geron, and T. Pierce (1996), Isoprene fluxes measured by enclosure, relaxed eddy accumulation, surface layer gradient, mixed layer gradient, and mixed layer mass balance techniques, *J. Geophys. Res., 101*, (D13), 18555–18568.

Hübner, J (2010), Einsatzvorbereitung einer REA-Anlage über Wiesenflächen, Diploma Thesis, University of Bayreuth, Germany, http://www.bayceer.uni-bayreuth.de/mm/de/top/diss/88759/DA_Joerg_Huebner.pdf

Jordan, A., and W. A. Brand (2003), Technical Report: MPI-BGC, Germany, in *Report of the Eleventh WMO/IAEA Meeting of Experts on Carbon Dioxide Concentration and Related Tracer Measurement Techniques, Tokyo, Japan, Sept. 2001, WMO-GAW Report 148*, edited by S. Toru and S. Kazuto, pp. 149-153.

Kaplan, J. O., I. C. Prentice, and N. Buchmann (2002), The stable carbon isotope composition of the terrestrial biosphere: Modeling at scales from the leaf to the globe, *Glob. Biogeochem. Cycles, 16*, 1060, doi:10.1029/2001GB001403.

Katul, G. G., P. L. Finkelstein, J. F. Clarke, and T. G. Ellestad (1996), An investigation of the conditional sampling method used to estimate fluxes of active, reactive, and passive scalars, *J. Appl. Meteor.*, *35*, 1835-1845.

Kramm, G., N. Beier, R. Dlugi, and H. Muller (1999), Evaluation of conditional sampling methods, *Contr. Atmos. Phys.*, *72*, 161-172.

Lee, X. (2000), Water vapor density effect on measurements of trace gas mixing ratio and flux with a massflow controller, *J. Geophys. Res.*, *105*, (D14), 17807-17810.

Lenschow, D. H., and M. R. Raupach (1991), The attenuation of fluctuatations in scalar concentrations through sampling tubes, *J. Geophys. Res.*, *96*, (D8), 15259-15268.

Leuning, R., and M. J. Judd (1996), The relative merits of open- and closed-path analysers for measurement of eddy fluxes, *Global Change Biol.*, *2*, 241-253.

Lloyd, J., and G. D. Farquhar (1994), ^{13}C discrimination during CO_2 assimilation by the terrestrial biosphere, *Oecologia*, *99*, 201-215.

Lloyd, J., B. Kruijt, D. Y. Hollinger, J. Grace, R. J. Francey, S. C. Wong, F. M. Kelliher, A. C. Miranda, G. D. Farquhar, J. H. C. Gash, N. N. Vygodskaya, I. R. Wright, H. S. Miranda, and E. D. Schulze (1996), Vegetation effects on the isotopic composition of atmospheric CO_2 at local and regional scales: Theoretical aspects and a comparison between rain forest in Amazonia and a Boreal Forest in Siberia, *Austr. J. Plant Physiol.*, *23*, 371-399.

Massman, W. J. (1991), The attenuation of concentration fluctuations in turbulent flow through a tube, *J. Geophys. Res.*, *96*, (D8), 15269-15273.

Mauder, M., and T. Foken (2004), Documentation and instruction manual of the eddy covariance software package TK2, *Arbeitsergebnisse 26*, 45 pp, Universität Bayreuth, Abt. Mikrometeorologie, Bayreuth, Germany. Print, ISSN 1614-8916.

McInnes, K. J., C. S. Campbell, and J. L. Heilman (1998), Separation and dispersion of conditionally sampled eddies through an intake tube, *Agron. J.*, *90*, 845-850.

Miller, J. B. (Ed.) (2006), *13th WMO/IAEA Meeting of Experts on Carbone Dioxide Concentration and Related Tracers Measurement Techniques, Boulder, Colorado, USA, Sept. 2005, WMO-GAW Report 168*, 201 pp.

Milne, R., A. Mennim, and K. Hargreaves (2001), The value of the beta coefficient in the relaxed eddy accumulation method in terms of fourth-order moments, *Boundary-Layer Meteorol.*, *101*, 359-373.

Moncrieff, J. B., I. J. Beverland, D. H. O'Neill, and F. D. Cropley (1998), Controls on trace gas exchange observed by a conditional sampling method, *Atmos. Environ.*, *32*, 3265-3274.

Oncley, S. P., A. C. Delany, T. W. Horst, and P. P. Tans (1993), Verification of flux measurement using relaxed eddy accumulation, *Atmos. Environ.*, *27A*, 2417-2426.

Pattey, E., R. L. Desjardins, F. Boudreau, and P. Rochette (1992), Impact of density fluctuations on flux measurements of trace gases: implications for the relaxed eddy accumulation technique, *Boundary-Layer Meteorol.*, *59*, 195-203.

Pattey, E., R. L. Desjardins, and P. Rochette (1993), Accuracy of the relaxed eddy-accumulation technique, evaluated using CO_2 flux measurements, *Boundary-Layer Meteorol.*, *66*, 341-355.

Rothe, M., A. Jordan, and W. A. Brand (2005), Trace gases, δ^{13}C and δ^{18}O of CO_2-in-air samples: Storage in glass flasks using PCTFE seals and other effects, in *Proceedings of the 12th WMO/IAEA Meeting of Expert on Carbon Dioxide Concentration and Related Tracers Measurements Techniques, Toronto, Canada, Sept. 2003, WMO-GAW Report 161*, edited by D. Worthy and L. Huang, pp. 64-70.

Ruppert, J., B. Wichura, A. C. Delany, and T. Foken (2002), Eddy sampling methods, a comparison using simulation results, paper presented at 15th Symposium on Boundary Layers an Turbulence, American Meteorological Society, Wageningen, Netherlands, 15-19 July 2002.

Ruppert, J. (2005), ATEM software for atmospheric turbulent exchange measurements using eddy covariance and relaxed eddy accumulation systems + Bayreuth whole-air REA system setup, *Arbeitsergebnisse 28*, 29 pp, Universität Bayreuth, Abt. Mikrometeorologie, Bayreuth, Germany. Print, ISSN 1614-8916.

Ruppert, J., and T. Foken (2005), Messung turbulenter Flüsse von Kohlendioxid und stabilem Kohlenstoffisotop ^{13}C über Pflanzenbeständen mit Hilfe der Relaxed Eddy Accumulation Methode, in Klimatologische und mikrometeorologische Froschungen im Rahmen des Bayreuther Institutes für terrestrische Ökosystemforschung (BITÖK) 1998 - 2004, edited by T. Foken, *Arbeitsergebnisse 29*, 81-104, Universität Bayreuth, Abt. Mikrometeorologie, Bayreuth, Germany. Print, ISSN 1614-8916.

Ruppert, J., M. Mauder, C. Thomas, and J. Lüers (2006a), Innovative gap-filling strategy for annual sums of CO_2 net ecosystem exchange, *Agric. For. Meteorol., 138*, 5-18, doi:10.1016/j.agrformet.2006.03.003.

Ruppert, J., C. Thomas, and T. Foken (2006b), Scalar similarity for relaxed eddy accumulation methods, *Boundary-Layer Meteorol., 120*, 39-63, doi:10.1007/s10546-005-9043-3.

Ruppert, J (2009), CO_2 and Isotope Flux Measurements above a Spruce Forest, PhD-Thesis, University of Bayreuth, http://opus.ub.uni-bayreuth.de/volltexte/2009/541/

Schauer, A. J., C. T. Lai, D. R. Bowling, and J. R. Ehleringer (2003), An automated sampler for collection of atmospheric trace gas samples for stable isotope analyses, *Agric. For. Meteorol., 118*, 113-124, doi:10.1016/S0168-1923(03)00065-0.

Staudt, K., and T. Foken (2007), Documentation of reference data for the experimental areas of the Bayreuth Centre for Ecology and Environmental Research (BayCEER) at the Waldstein site, *Arbeitsergebnisse 35*, 37 pp, Universität Bayreuth, Abt. Mikrometeorologie, Bayreuth, Germany. Print, ISSN 1614-8916.

Sturm, P., M. Leuenberger, C. Sirignano, R. E. M. Neubert, H. A. J. Meijer, R. Langenfelds, W. A. Brand, and Y. Tohjima (2004), Permeation of atmospheric gases through polymer O-rings used in flasks for air sampling, *J. Geophys. Res., 109*, D04309, doi:10.1029/2003JD004073.

Thomas, C., J. Ruppert, J. Lüers, J. Schröter, J. C. Mayer, and T. Bertolini (2004), Documentation of the WALDATEM-2003 experiment, 28.4.-3.8.2003, *Arbeitsergebnisse 24*, 59 pp, Universität Bayreuth, Abt. Mikrometeorologie, Bayreuth, Germany. Print, ISSN 1614-8916.

Thomas, C., and T. Foken (2007), Organised Motion in a Tall Spruce Canopy: Temporal Scales, Structure Spacing and Terrain Effects, *Boundary-Layer Meteorol., 122*, 123-147, doi:10.1007/s10546-006-9087-z.

Webb, E. K., G. I. Pearman, and R. Leuning (1980), Correction of flux measurements for density effects due to heat and water vapour transfer, *Quart. J. Roy. Meteor. Soc., 106*, 85-100.

Werner, R. A., and W. A. Brand (2001), Referencing strategies and techniques in stable isotope ratio analysis, *Rapid Commun. Mass Spectrom., 15*, 501-519.

Werner, R. A., M. Rothe, and W. A. Brand (2001), Extraction of CO_2 from air samples for isotopic analysis and limits to ultra high precision delta O-18 determination in CO_2 gas, *Rapid Commun. Mass Spectrom., 15*, 2152-2167.

Wichura, B., N. Buchmann, and T. Foken (2000), Fluxes of the stable carbon isotope ^{13}C above a spruce forest measured by hyperbolic relaxed eddy accumulation method, paper presented at 14th Symposium on Boundary Layers and Turbulence, American Meteorological Society, Boston, Aspen, Colorado, 7-11 August 2000.

Wichura, B; Ruppert, J; Delany, AC; Buchmann, N; Foken, T: Structure of carbon dioxide exchange processes above a spruce forest, Matzner, E.: Ecological Studies, Biogeochemistry of forested catchments in a changing environment: a German case study, Springer Verlag, 172, 161-176 (2004)

Wichura, B: Untersuchungen zum Kohlendioxid-Austausch über einem Fichtenwaldbestand; Hyperbolic-Relaxed-Eddy-Accumulation Messungen für das stabile Kohlenstoffisotop ^{13}C und Waveletanalysen des turbulenten Kohlendioxid-Austausches, Bayreuther Institut für Terrestrische Ökosystemforschung (BITÖK): *Bayreuther Forum Ökologie, Selbstverlag, 114*, 295 S. (2009)

Wilczak, J. M., S. P. Oncley, and S. A. Stage (2001), Sonic anemometer tilt correction algorithms, *Boundary-Layer Meteorol., 99*, 127-150.

Wyngaard, J. C., and C.-H. Moeng (1992), Cospectral similarity in the atmospheric surface layer, *Quart. J. Roy. Meteor. Soc., 98*, 590-603.

Yakir, D., and X.-F. Wang (1996), Fluxes of CO_2 and water between terrestrial vegetation and the atmosphere estimated from isotope measurements, *Nature, 380*, 515-517.

Yakir, D., and L. da S. L. Sternberg (2000), The use of stable isotopes to study ecosystem gas exchange, *Oecologia, 123*, 297-311.

Zobitz, J. M., J. P. Keener, H. Schnyder, and D. R. Bowling (2006), Sensitivity analysis and quantification of uncertainty for isotopic mixing relationships in carbon cycle research, *Agric. For. Meteorol., 136*, 56-75, doi:10.1016/j.agrformet.2006.01.003.

Volumes in the series 'University of Bayreuth, Department of Micrometeorology, Arbeitsergeb-nisse'

Nr	Author(s)	Title	Year
01	Foken	Der Bayreuther Turbulenzknecht	01/1999
02	Foken	Methode zur Bestimmung der trockenen Deposition von Bor	02/1999
03	Liu	Error analysis of the modified Bowen ratio method	02/1999
04	Foken et al.	Nachfrostgefährdung des ÖBG	03/1999
05	Hierteis	Dokumentation des Experimentes Dlouhá Louka	03/1999
06	Mangold	Dokumentation des Experimentes am Standort Weidenbrunnen, Juli/August 1998	07/1999
07	Heinz et al.	Strukturanalyse der atmosphärischen Turbulenz mittels Wavelet-Verfahren zur Bestimmung von Austauschprozessen über dem antarktischen Schelfeis	07/1999
08	Foken	Comparison of the sonic anemometer Young Model 81000 during VOITEX-99	10/1999
09	Foken et al.	Lufthygienisch-bioklimatische Kennzeichnung des oberen Egertales, Zwischenbericht 1999	11/1999
10	Sodemann	Stationsdatenbank zum BStMLU-Projekt Lufthygienisch-bioklimatische Kennzeichnung des oberen Egertales	03/2000
11	Neuner	Dokumentation zur Erstellung der meteorologischen Eingabedaten für das Modell BEKLI-MA	10/2000
12	Foken et al.	Dokumentation des Experimentes VOITEX-99	10/2000
13	Bruckmeier et al.	Documentation of the experiment EBEX-2000, July 20 to August 24, 2000	01/2001
14	Foken et al.	Lufthygienisch-bioklimatische Kennzeichnung des oberen Egertales	02/2001
15	Göckede	Die Verwendung des Footprint-Modells nach Schmid (1997) zur stabilitätsabhängigen Bestimmung der Rauhigkeitslänge	03/2001
16	Neuner	Berechnung der Evaporation im ÖBG (Universität Bayreuth) mit dem SVAT-Modell BEKLIMA	05/2001
17	Sodemann	Dokumentation der Software zur Bearbeitung der FINTUREX-Daten	08/2002
18	Göckede et al.	Dokumentation des Experiments STINHO-1	08/2002
19	Göckede et al.	Dokumentation des Experiments STINHO-2	12/2002
20	Göckede et al	Characterisation of a complex measuring site for flux measurements	12/2002
21	Liebethal	Strahlungsmessgerätevergleich während des Experiments STINHO-1	01/2003

22	Mauder et al.	Dokumentation des Experiments EVA_GRIPS	03/2003
23	Mauder et al.	Dokumentation des Experimentes LITFASS-2003, Dokumentation des Experimentes GRASATEM-2003	12/2003
24	Thomas et al.	Documentation of the WALDATEM-2003 Experiment	05/2004
25	Göckede et al.	Qualitätsbegutachtung komplexer mikrometeorologischer Messstationen im Rahmen des VERTIKO-Projekts	11/2004
26	Mauder & Foken	Documentation and instruction manual of the eddy covariance software package TK2	12/2004
27	Herold et al.	The OP-2 open path infrared gas analyser for CO_2 and H_2O	01/2005
28	Ruppert	ATEM software for atmospheric turbulent exchange measurements using eddy covariance and relaxed eddy accumulation systems and Bayreuth whole-air REA system setup	04/2005
29	Foken (Ed.)	Klimatologische und mikrometeorologische Forschungen im Rahmen des Bayreuther Institutes für Terrestrische Ökosystemforschung (BITÖK), 1989-2004	06/2005
30	Siebicke & Serafimovich	Ultraschallanemometer-Überprüfung im Windkanal der TU Dresden 2007	04/2007
31	Lüers & Bareiss	The Arctic Turbulence Experiment 2006 PART 1: Technical documentation of the ARCTEX 2006 campaign, May, 2nd to May, 20th 2006	07/2007
32	Lüers & Bareiss	The Arctic Turbulence Experiment 2006 PART 2: Visualization of near surface measurements during the ARCTEX 2006 campaign, May, 2nd to May, 20th 2006	07/2007
33	Bareiss & Lüers	The Arctic Turbulence Experiment 2006 PART 3: Aerological measurements during the ARCTEX 2006 campaign, May, 2nd to May, 20th 2006	07/2007
34	Metzger & Foken et al.	COPS experiment, Convective and orographically induced precipitation study, 01 June 2007 – 31 August 2007, Documentation	09/2007
35	Staudt & Foken	Documentation of reference data for the experimental areas of the Bayreuth Centre for Ecology and Environmental Research (BayCEER) at the Waldstein site	11/2007
36	Serafimovich et al.	ExchanGE processes in mountainous Regions (EGER) - Documentation of the Intensive Observation Period (IOP1), September, 6th to October, 7th 2007	01/2008
37	Serafimovich et al.	ExchanGE processes in mountainous Regions (EGER) - Documentation of the Intensive Observation Period (IOP2), June, 1st to July, 15th 2008	10/2008
38	Siebicke	Footprint synthesis for the FLUXNET site Waldstein/Weidenbrunnen (DE-Bay) during the EGER experiment.	12/2008
39	Lüers & Foken	Jahresbericht 2008 zum Förderprojekt 01879 - Untersuchung der Veränderung der Konzentration von Luftbeimengungen und Treibhausgasen im hohen Fichtelgebirge 2007 – 2013	01/2009
40	Lüers & Foken (Eds.)	Proceedings of the International Conference of "Atmospheric Transport and Chemistry in Forest Ecosystems" Castle of Thurnau, Germany, Oct 5 to Oct 8, 2009	10/2009
41	Biermann et al.	Mesoscale circulations and energy and gas exchange over the Tibetan Plateau – Documentation of the micrometeorological experiment, Nam Tso, Tibet , 25 June 2009 – 08 August 2009	12/2009

42	Foken & Falke	Documentation and Instruction Manual for the Krypton Hygrometer Calibration Instrument	01/2010 Update: 12/2011
43	Lüers & Foken	Jahresbericht 2009 zum Förderprojekt 01879 - Untersuchung der Veränderung der Konzentration von Luftbeimengungen und Treibhausgasen im hohen Fichtelgebirge 2007 – 2013	07/2010
44	Biermann et al.	Tibet Plateau Atmosphere-Ecology-Glaciology Cluster Joint *Kobresia* Ecosystem Experiment: Documentation of the first Intensive Observation Period (IOP 1) summer 2010 in Kema, Tibet	01/2011
45	Zhao et al.	Complex TERRain and ECOlogical Heterogeneity (TERRECO);WP 1-02: Spatial assessment of atmosphere-ecosystem exchanges via micrometeorological measurements, footprint modeling and mesoscale simulations ; Documentation of the Observation Period May 12th to Nov. 8th, 2010, Haean, South Korea	03/2011
46	Mauder & Foken	Documentation and Instruction Manual of the Eddy-Covariance Software Package TK3	05/2011
47	Serafimovich et al.	ExchanGE processes in mountainous Regions (EGER)- Documentation of the Intensive Observation Period (IOP3) June, 13t^{h} to July, 26th 2011	11/2011
48	Hübner et al.	Documentation and Instruction Manual for the Horizontal Mobile Measuring System (HMMS)	12/2011
49	Lüers et al.	The Arctic Turbulence Experiment 2009 - additional laser Scintillometer measurement campaign 2009 at the Bayelva catchment on Svalbard: Technical documentation and visualization of the near surface measurements during the ARCTEX-2009 campaign, August, 10th to August, 20th 2009	02/2012
50	Foken	Klimawanderweg auf der Landesgartenschau in Bamberg 2012	04/2012
51	Ruppert et al.	Whole-air relaxed eddy accumulation for the measurement of isotope and trace-gas fluxes	06/2012